Do NAD and NAT Form in Liquid Stratospheric Aerosols by Pseudoheterogeneous Nucleation?

Daniel A. Knopf*,†

Institute for Atmospheric and Climate Science, IAC, ETH Zürich, Zürich, Switzerland

Received: September 21, 2005; In Final Form: January 24, 2006

Laboratory data of the freezing of nitric acid hydrates (NAD, NAT) from HNO_3/H_2O and $HNO_3/H_2SO_4/H_2O$ solution droplets have been evaluated with respect to a "pseudoheterogeneous" (surface-induced) nucleation mechanism of NAD and NAT, which has been argued to possibly lead to the formation of polar stratospheric clouds (PSCs). In addition, a parametrization of pseudoheterogeneous nucleation of NAD and NAT suggested recently (Tabazadeh et al. *J. Phys. Chem. A* **2002**, *106*, 10238−10246) has been analyzed, showing that this parametrization should not be used in stratospheric modeling studies. The analysis of several laboratory data sets yields an upper limit of the pseudoheterogeneous nucleation rate coefficient of NAD of 2.2×10^{-5} cm^{-2} s^{-1}. In contrast, the upper limit of the pseudoheterogeneous nucleation rate coefficient of NAT could not be constrained satisfactorily, since formation of NAT has not been observed at stratospheric conditions in laboratory experiments applying small droplets. Maximum NAD production rates of 9.6×10^{-9} cm^{-3} (air) h^{-1} in the stratosphere have been estimated assuming a pseudoheterogeneous nucleation mechanism that is constrained by the experimental observations. If maximum NAD supersaturation persisted for 4 weeks in the polar stratosphere the corresponding NAD particle number densities are estimated to be about 6×10^{-6} cm^{-3}. These particle number densities are 3 orders of magnitude lower than particle number densities recently observed in the stratosphere. In conclusion, on the basis of laboratory data it is found that a pseudoheterogeneous nucleation mechanism is not sufficient to explain recent observations of large nitric acid containing particles in the polar stratosphere.

Introduction

Polar stratospheric clouds (PSCs) convert halogen reservoir species into active species, which can effectively destroy ozone. Nitric acid trihydrate (NAT) particles and supercooled ternary solution (STS) droplets have been observed within PSCs.[1−4] Nitric acid dihydrate (NAD) particles have been suggested as possible PSC particles based on laboratory experiments.[5,6] Recently, large nitric acid containing particles, 2−22 μm in diameter, with particle number densities of up to 10^{-3} cm^{-3} have been observed,[7−9] which can lead to an efficient denitrification in the polar vortex, intensifying ozone destruction.

The formation mechanism of NAD and NAT particles in the polar stratosphere is still not resolved. Tabazadeh and coworkers[10−13] suggested recently that a so-called "pseudoheterogeneous" nucleation mechanism, representing a nucleation mechanism occurring at the particle surface instead of in the bulk, leads to the nucleation in cloud particles. The pseudoheterogeneous nucleation rate coefficient should then depend on the surface area of the particle instead of on the volume as is the case in classical nucleation theory.[10] The evidence of pseudoheterogeneous nucleation is still under discussion (see, e.g., Kay et al.[14] and Koop[15]). Attempts have been made to study this newly suggested nucleation mechanism. Khvorostyanov and Curry[16] implemented pseudoheterogeneous nucleation in generalized classical nucleation theory to improve the understanding of the freezing process. Molecular dynamics simulation applying SeF_6 clusters indicated that nucleation can take place at the surface.[17,18] One of these studies showed that nucleation may be better described by a surface-based nucleation process[17] whereas the other study found that nucleation occurred occasionally at the surface but more often in the volume.[18] Stöckel et al.[19] and Duft and Leisner[20] showed experimentally that the freezing of supercooled water droplets was due to a volume-based nucleation process. However, these experiments used droplets in the size ranges of 19−85 μm[19,20] and the question remains if this result still holds for smaller particles.

In the search of the formation mechanism of NAD and NAT particles in the polar stratosphere Knopf et al.[21] showed, based on several laboratory data sets,[21−27] that homogeneous nucleation rates of NAD and NAT from STS droplets are too low to account for the formation of large nitric acid containing particles. Recently, Tabazadeh et al.[10] suggested that the formation of NAD and NAT was due to pseudoheterogeneous nucleation. Additionally, these authors presented a parametrization for implementation in stratospheric modeling studies to simulate the formation of NAD and NAT by pseudoheterogeneous nucleation. This parametrization has been applied in several modeling studies showing inconsistencies in reproducing field data.[28−33] In some of these studies the NAD particle production rates derived from the parametrization had to be corrected by 1−2 orders of magnitude to lower values[30,32,33] or the activation energy to form a critical cluster to initiate the crystallization had to be increased.[31] However, the study of Pagan et al.[34] suggested that pseudoheterogeneous nucleation cannot be ruled out when possible temperature uncertainties in the applied temperature fields of the models are considered.

Here, a reinvestigation of various laboratory data sets concerned with the formation of NAD and NAT from binary

* Address correspondence to the author at e-mail knopf@chem.ubc.ca.
† Present address: Department of Chemistry, University of British Columbia, British Columbia, Canada.

10.1021/jp055376j CCC: $33.50
Published on Web 04/12/2006

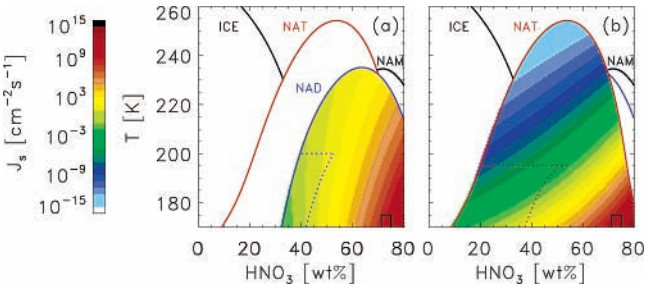

Figure 1. Pseudoheterogeneous nucleation rate coefficients of NAD (a) and NAT (b) in binary HNO_3/H_2O solutions as a function of temperature and concentration calculated from the formulation of Tabazadeh et al.[10] Solid lines show the melting point curves of the different solid phases ($S = 1$). The regions between dotted and solid lines indicate typical polar stratospheric temperatures ($\leq$200 K) and saturation ratios ($S_{NAD} \leq 4.7$ and $S_{NAT} \leq 23.5$ for NAT). The solid square marks the temperature and concentration range in which Bertram et al.[26] did not observe nucleation in submicron HNO_3/H_2O particles.

HNO_3/H_2O and ternary $HNO_3/H_2SO_4/H_2O$ solution droplets[21−27,35−37] is presented. This analysis will show that pseudoheterogeneous nucleation is not sufficient to explain the particle number densities observed in the polar stratosphere. In addition, the parametrization suggested by Tabazadeh et al.[10] is analyzed, indicating that it is not suitable to be applied in stratospheric modeling studies.

Nucleation Formulation Analysis

Tabazadeh et al.[10] derived the following equation for the pseudoheterogeneous nucleation rate coefficient:

$$J_S(T) = N_S\left(\frac{kT}{h}\right)\exp\left[\frac{-\Delta G^S_{act}(T)}{RT}\right] \quad (1)$$

where N_S is the number of HNO_3 molecules per unit surface area of the liquid (i.e., $N_S = X_{HNO_3} \cdot n_S$, where X_{HNO_3} is the mole fraction of HNO_3 in the bulk liquid and $n_S = 10^{15}$ cm^{-2} is an approximate number of surface sites on the liquid surface), R is the universal gas constant, k is the Boltzmann constant, h is the Planck constant, T is the temperature, and ΔG^S_{act} is the activation energy required to form a critical cluster on the droplet surface. Tabazadeh et al.[10] presented a parametrization to determine ΔG^S_{act} for the formation of NAD and NAT by pseudoheterogeneous nucleation (see eqs 6−8 in Tabazadeh et al.[10]). These ΔG^S_{act} values can be used to calculate pseudoheterogeneous nucleation rate coefficients, J_S, using eq 1 as a function of HNO_3 and H_2O concentration and temperature. Figure 1 shows the resulting pseudoheterogeneous nucleation rate coefficients. The following deficiencies arise applying this parametrization:

First, this parametrization produces finite values of J_S at the melting points of NAD and NAT (solid lines in Figure 1, where the saturation ratio $S_{NAX} = 1$, X = D, T). This is thermodynamically not reasonable since it implies that a solid NAD or NAT crystal would not melt at its melting point. The pseudoheterogeneous nucleation rate coefficient must decrease to zero when approaching $S_{NAX} = 1$. Second, the pseudoheterogeneous nucleation rate coefficient of NAD does not change significantly in a temperature range of 200 to 170 K at stratospheric conditions (between the solid and dotted lines in Figure 1a), although supersaturation with respect to NAD increases from 1.1 to 3.5. This is in contrast to laboratory observations which indicate that a change in S_{NAX} results in a significant change in J_S.[21−27,35] Third, the parametrization predicts the highest J_S values at conditions for which Bertram et al.[26] did not observe nucleation in submicron HNO_3/H_2O droplets (solid squares in Figure 1). Assuming an uncertainty of the suggested parametrization of about half an order of magnitude[10] (which is based on a similar uncertainty of the experimental data sets) the nucleation data of Bertram et al.[26] can be reproduced for HNO_3 concentrations of up to 65 wt % by the parametrization. However, for higher HNO_3 concentrations (solid squares in Figure 1) the parametrization is in disagreement with the laboratory data.

For these reasons, it is strongly recommended that this parametrization should not be used in stratospheric modeling studies.

Experimental Results and Discussion

In the following the data obtained and used by Knopf et al.[21] and the data of Disselkamp et al.,[35] Anthony et al.,[36] and Prenni et al.[37] are inspected with respect to pseudoheterogeneous nucleation. This analysis is conducted under the following assumptions which apply to all data sets used in this study:[21−27,35−37] (1) There are no significant amounts of surfactants on the surface of the droplets and bulk volumes which could hinder the pseudoheterogeneous nucleation process.[13,38] (2) The excess surface coverage of nitric acid at the surface of the droplets does not differ for the various particle sizes applied in this study. The latter is in accordance with the work of Djikaev and Tabazadeh,[39] who showed that the excess surface coverage of nitric acid does not change significantly for droplet radii >0.03 μm. The radii of the particles of the applied experimental data sets[21,24−27,35−37] range from 0.33 μm to 1.3 mm.

In the following the derivation of the pseudoheterogeneous nucleation rate coefficient, J_S, and the corresponding activation energy to form a critical cluster at the air−liquid surface, ΔG^S_{act}, for the applied data sets are given. An upper limit of the pseudoheterogeneous nucleation rate coefficient, J^{up}_S, for the experimental data sets of Knopf et al.[21] (large droplet data) and Koop et al.[22,23] (bulk experiments of about 1 cm^3 in volume) was obtained by applying the equation

$$J^{up}_S(T) = \frac{n^*}{\sum_i A_i \cdot t_i(T)} \quad (2)$$

where $t_i(T) = \int_T^{T_i^*} (dT/dt)_i^{-1}\, dT$ is the time interval that the ith droplet or bulk volume with surface A_i remained liquid between T and T_i^*. T_i^* is either the nucleation temperature of the droplet or the lowest investigated temperature (i.e., in the case in which the formation of a solid phase has not been observed), and $(dT/dt)_i$ is the cooling rate applied in the particular experiment. A_i indicates the air−liquid surface of the droplets or bulk volumes. n^* is the upper fiducial limit of n determined by Poisson statistics at a confidence level of 0.999,[23] i.e., if the experiments were repeated an infinite number of times the observed number of nucleation events will be smaller than n^* in 99.9% of the cases. n^* is always larger than n and, therefore, $J^{up}_S(T)$ represents an upper limit of J_S. $J^{up}_S(T)$ also represents a conservative value for the following reasons. The time interval, $t_i(T)$, that a droplet stays liquid below T is always smaller than the time interval it would stay liquid at T. This assumes that $J^{up}_S(T)$ monotonically increases as T decreases for the investigated temperature range. Additionally, for larger sample volumes heterogeneous nucleation cannot be entirely ruled out. Hetero-

geneous nucleation by a solid impurity such as a dust particle, for example, is more efficient than pseudoheterogeneous nucleation since a preexisting solid most likely lowers the activation barrier to form a critical cluster.[40] Such an "artificial" increase in the pseudoheterogeneous nucleation rate coefficient is considered by applying an upper limit of J_S.

The derived J_S^{up} values were used to calculate lower limits of the activation energy for the formation of a critical cluster, $\Delta G_{act}^{S,low}$, after solving eq 1 for ΔG_{act}^{S}:

$$\Delta G_{act}^{S,low}(T) = -RT \ln\left[\frac{h}{kT}\frac{J_S^{up}(T)}{N_S}\right] \quad (3)$$

The nucleation experiments of Anthony et al.[36] have been considered in this study. To obtain J_S, first J_V has to be derived.[10] An estimate of the homogeneous nucleation rate coefficient, J_V, of the ternary $H_2SO_4/HNO_3/H_2O$ aerosol data of Anthony et al.[36] has been derived by using the following equation as given by the authors

$$J_V < \frac{0.05}{t \cdot \mathrm{vol}} \quad (4)$$

where t is the time the aerosol particles stayed at $T_{initial}$ representing the lowest temperature studied in the experiment. t has been taken as 30 min (see Table 1 of Anthony et al.[36]). vol is the volume of an aerosol particle 0.7 μm in diameter. The factor of 0.05 represents the detection limit of the instrumental setup to observe nucleation. No nucleation of NAD and NAT has been observed in these studies. For this reason the evaluated J_V values represent upper limits.

J_S values for the data of Disselkamp et al.,[35] Anthony et al.,[36] Prenni et al.,[37] Bertram and Sloan,[24,25] Bertram et al.,[26] and Salcedo et al.[27] were obtained by applying the analysis of Tabazadeh et al.:[10] J_S was calculated using $J_S = (r/3)J_V$, where r is the radius of the droplet and J_V is the homogeneous nucleation rate coefficient.[10] For the data sets of Disselkamp et al.,[35] Anthony et al.,[36] Prenni et al.,[37] Bertram and Sloan,[24,25] and Salcedo et al.[27] droplet sizes of about 1.5, 0.7, 1, 0.76, and 50 μm, respectively, were applied.[10] For the data set of Bertram et al.[26] a surface median diameter of 0.66 μm and a homogeneous nucleation rate coefficient of $J_V = 4.4 \times 10^9$ cm^{-3} s^{-1} were used (A. K. Bertram, personal communication).

The derived J_S values were used to derive ΔG_{act}^{S} by applying eq 3. This procedure resulted in ΔG_{act}^{S} values as a function of nucleation temperature and saturation ratio for the individual experiments. Figure 2 represents these ΔG_{act}^{S} values as a function of temperature and S_{NAX}. Since also upper limits of J_S^{up}, and thus lower limits of $\Delta G_{act}^{S,low}$, have been employed, the evaluated data represent conservative lower limits of the ΔG_{act}^{S}. For this reason, the actual ΔG_{act}^{S} must be larger than the values shown in Figure 2, which results in actual lower J_S values. Additionally, in Figure 2 the stratospheric relevant regime is indicated by the blue and orange lines. It should be kept in mind that a high ΔG_{act}^{S} value corresponds to a low J_S value and vice versa (see eq 1). This has implications for the analysis of these data sets. For example, in the case of heterogeneous nucleation by an impurity, an overestimation of J_S and, thus, an underestimation of ΔG_{act}^{S} would result. Therefore, for one specific experimental temperature the highest ΔG_{act}^{S} value corresponds most likely to a purely pseudoheterogeneous nucleation process. The ΔG_{act}^{S} values obtained with use of the parametrization by Tabazadeh et al.[10] are also shown in Figure 2 as dashed lines. Although it has been shown in the previous section that the parametrization is erroneous the results of the parametrization are plotted in Figure 2 for analytical purposes. The parametrization of Tabazadeh et al.[10] produces significantly smaller ΔG_{act}^{S} values in the case of NAD nucleation (Figure 2a) than the ones obtained from the various experiments at stratospheric conditions. As discussed above, the actual ΔG_{act}^{S} values have to be higher than the experimentally obtained values, clearly indicating that the parametrization is erroneous in the stratospherically relevant regime. In the case of NAT nucleation (Figure 2b) the parametrization is in agreement with the experimentally obtained $\Delta G_{act}^{S,low}$ values at stratospheric conditions since it produces more conservative ΔG_{act}^{S} values than the ones obtained by the analysis of the experimental data. The presented differences in the ΔG_{act}^{S} values derived from the parametrization and experimental data are significant. An underestimation of ΔG_{act}^{S} by 1 kcal mol^{-1} increases the pseudoheterogeneous nucleation rate coefficient by a factor of 14, which is 3 times higher than the uncertainty in most data and parametrizations.[10]

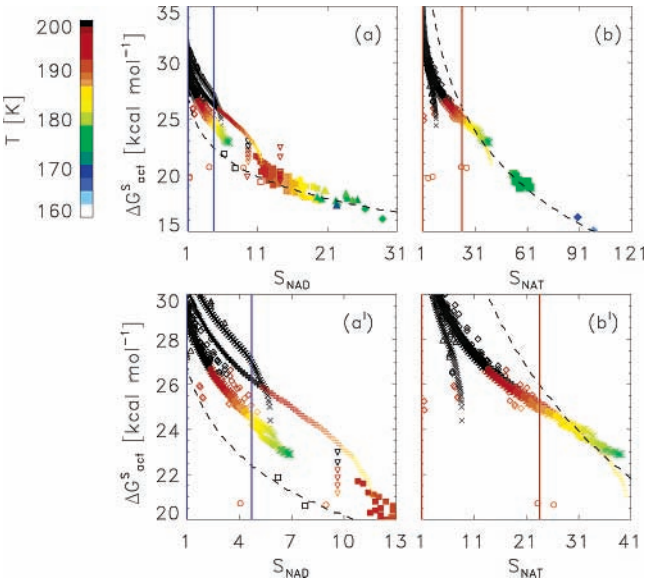

Figure 2. ΔG_{act}^{S} is given as a function of the NAD and NAT saturation ratios derived from laboratory nucleation data. Large droplet data: (×) 63.6 wt % HNO_3; (+) 53.8 wt % HNO_3; (∗) 32.2 wt HNO_3 and 13.8 wt % H_2SO_4; and (●) 38.3 wt % HNO_3 and 7.6 wt % H_2SO_4.[21] Bulk solution data: (△) binary HNO_3/H_2O solutions of varying composition;[23] (◇) ternary $HNO_3/H_2SO_4/H_2O$ solutions of varying composition.[22,23] Aerosol data: (a) (■) 57, 60, and 64 wt % HNO_3,[27] (□) 64 wt % HNO_3,[35] (▽) 54, 58, and 64 wt % HNO_3,[37] (○) ternary $HNO_3/H_2SO_4/H_2O$ solutions of varying composition,[36] (◆) 64 wt % HNO_3,[24] (▲) binary HNO_3/H_2O aerosol of varying composition;[26] (b) (■) 54 wt % HNO_3,[27] (◆) 54 wt % HNO_3,[25] (○) ternary $HNO_3/H_2SO_4/H_2O$ solutions of varying composition.[36] The color coding indicates at which temperature the data were obtained. Dashed lines indicate ΔG_{act}^{S} values derived by using the parametrization of Tabazadeh et al.[10] applying $X_{HNO_3} = 0.333$ and 0.246 for NAD (a) and NAT (b), respectively. Panels a′ and b′ show an enlarged view of the top left corner of panels a and b, respectively.

The experimentally derived ΔG_{act}^{S} values shown in Figure 2 also represent lower limits with respect to a possible enrichment of HNO_3 at the surface of the particle or bulk liquid.[41] From eq 3 it is conceivable that an increase of the HNO_3 surface concentration (i.e., an increase in N_S) leads to a higher value of ΔG_{act}^{S} for a fixed J_S value, which has been obtained from the experiment. Therefore, an increase in ΔG_{act}^{S} due to HNO_3 surface enrichment is also in agreement with the estimated lower limits of $\Delta G_{act}^{S,low}$ shown in Figure 2.

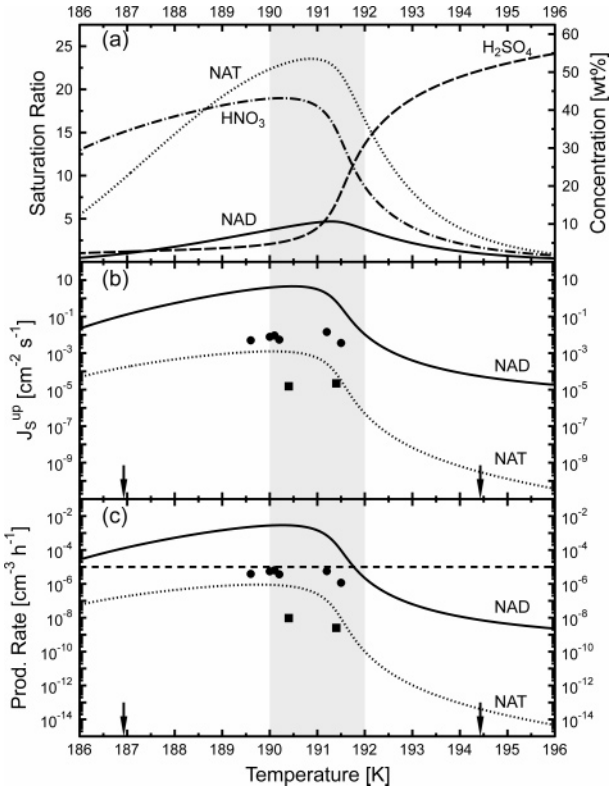

Figure 3. Panel a shows the composition (dashed and dashed-dotted lines) and the saturation ratios (solid and dotted lines) of STS aerosols as a function of temperature at 50 mbar with 5 ppmv H_2O, 10 ppbv HNO_3, and 0.5 ppbv H_2SO_4.[42] The shaded region indicates the temperature range where the S_{NAX} values reach a maximum. Panel b shows upper limits for the pseudoheterogeneous nucleation rate coefficients of NAD (squares) and NAT (circles) in STS droplets, derived from experimental data for the conditions shown in panel a. For comparison, solid and dotted lines indicate pseudoheterogeneous nucleation rate coefficients in STS droplets for the same conditions calculated, using the parametrization of Tabazadeh et al.[10] Panel c represents hourly production rates of NAD and NAT particles (squares and circles, respectively) per cm^3 of air derived from the nucleation rate coefficients shown in panel b. Also shown as solid and dotted lines are the NAD and NAT production rates for the same conditions calculated by using the formulation of Tabazadeh et al.[10] The black dashed line indicates the minimum hourly production rate ($\sim 10^{-5}$ cm^{-3}) to observe NAD and NAT particle number densities and subsequent polar denitrification.[10,45,46] Arrows in panels b and c mark the temperature where the saturation ratio of NAD equals one.

The combined data[21−27,35−37] were used to derive upper limits of the pseudoheterogeneous nucleation rate coefficients, J_S^{up}, under stratospherically relevant conditions. Figure 3a shows the composition of STS droplets at a height of 50 mbar for typical stratospheric mixing ratios of 5 ppmv H_2O, 10 ppbv HNO_3, and 0.5 ppbv H_2SO_4, and the corresponding saturation ratios with respect to NAD and NAT.[42] Figure 3b presents the experimentally obtained upper limits of the pseudoheterogeneous nucleation rate coefficients of NAD and NAT as squares and circles, respectively, for the conditions shown in panel a. J_S^{up} has been derived by selecting all available experimental data points in Figure 2 for one temperature and then interpolating these data as a function of saturation ratio S_{NAX}. The highest values of $\Delta G_{act}^{S,low}$ have been chosen (see discussion above) to obtain $\Delta G_{act}^{S,low}$ as a function of S_{NAX} for constant temperature. Then, for the chosen temperature, S_{NAX} was read off Figure 3a and used to derive the corresponding $\Delta G_{act}^{S,low}$ value, from which J_S^{up} with use of eq 1 was derived. The maximum experimentally obtained pseudoheterogeneous nucleation rate coefficients for NAD and NAT are 2.2×10^{-5} and 1.4×10^{-2} cm^{-2} s^{-1}, respectively. The pseudoheterogeneous nucleation rate coefficients for NAD and NAT derived from the parametrization of Tabazadeh et al. are also shown in Figure 3b as solid and dotted lines, respectively. The arrows in Figure 3b,c mark the temperature at which $S_{NAD} = 1$. At this temperature, i.e., the melting point of NAD, the pseudoheterogeneous nucleation rate coefficient must approach 0. It should be kept in mind that it has been shown above that the results of the parametrization are physically unreasonable (without the need of additional experimental data). However, the results of the parametrization are given in Figure 3 for comparison with the experimentally derived data, since under these stratospheric conditions the parametrization was applied in several modeling studies mentioned earlier.

The number of experimental data points in Figure 3b reflects the number of experiments with observed nucleation of NAD and NAT at temperatures between 190 and 192 K. However, Bertram and Sloan,[24,25] Bertram et al.,[26] Anthony et al.,[36] Prenni et al.,[37] and Salcedo et al.[27] did not observe NAT formation utilizing small droplets ($r \leq 25$ μm) at temperatures above 180 K (see Figure 2b). Therefore, the derivation of an upper limit of the pseudoheterogeneous nucleation rate coefficient of NAT could only be based on large droplet data[21] and bulk experiments.[22,23] As discussed above, heterogeneous nucleation may have occurred that may lead to an overestimation of J_S^{up}. For this reason, it is argued that the experimentally derived upper limits of the pseudoheterogeneous nucleation rate coefficients of NAT are not sufficiently constrained to be applied to stratospheric conditions. Laboratory studies have shown that the metastable NAD phase forms more readily than NAT.[5,6,26,43] For these reasons, the upper limit of the pseudoheterogeneous nucleation rate coefficient of NAT has to be lower than the one for NAD.

Figure 3c shows the experimentally derived hourly production rates of NAD and NAT particles in 1 cm^3 stratospheric air as squares and circles, respectively. The total particle surface area in 1 cm^3 stratospheric air was estimated by applying the observed particle volume[44] and by using a particle number density of about 10 cm^{-3}. The upper limits of the particle production rates of NAD and NAT obtained from the experimental data yield 9.6×10^{-9} and 6.4×10^{-6} cm^{-3} (air) h^{-1}, respectively. However, as discussed above, it should be kept in mind that the derived production rates of NAT are not well constrained and are given solely for the sake of completeness. The solid and dotted lines are NAD and NAT production rates, respectively, which were derived by using the parametrization given by Tabazadeh et al.[10] The dashed line indicates the minimum particle production rate ($\sim 10^{-5}$ cm^{-3} (air) h^{-1}) necessary to explain the observed particle number concentrations and subsequent denitrification of the polar vortex.[10,45,46]

The maximum experimentally obtained pseudoheterogeneous production rate of NAD is about 3 orders of magnitude lower than the minimum production rate necessary to explain the observed particle number densities and subsequent polar denitrification in stratospheric modeling studies.[10,45,46] In addition, the combined experimental data results in NAD production rates under stratospheric relevant conditions, which are about 5 orders of magnitude lower than the values obtained by the parametrization. This is a further corroboration that the proposed parametrization should not be applied at stratospheric conditions. This analysis of various NAD and NAT nucleation studies, which applied different aerosol sizes, indicates that pseudoheteroge-

neous nucleation does not play a significant role in the formation of solid nitric acid containing particles in the polar stratosphere.

Conclusions

The experimentally obtained upper limits of the pseudoheterogeneous nucleation rate coefficients for NAD and NAT yielded maximum values of 2.2×10^{-5} and 1.4×10^{-2} cm^{-2} s^{-1}, respectively. Applying the experimentally obtained upper limits of the pseudoheterogeneous nucleation rate coefficients to the stratosphere resulted in maximum production rates of 9.6×10^{-9} and 6.4×10^{-6} cm^{-3} (air) h^{-1} for NAD and NAT, respectively. As discussed above, the upper limits of the pseudoheterogeneous nucleation rate coefficients and production rates for NAT are not well constrained and are most likely not relevant for the stratosphere. This conclusion is corroborated by the fact that nucleation of NAT has not been observed in laboratory studies at stratospheric conditions applying small droplets.[24−27,36,37] This is in agreement with laboratory data showing that indeed NAD nucleates more readily than NAT.[5,6,26,43]

The maximum experimentally obtained pseudoheterogeneous production rate of NAD is about 3 orders of magnitude lower than the minimum production rate necessary to explain the observed polar denitrification in stratospheric modeling studies.[10,45,46] Applying the maximum NAD production rate and assuming that NAD supersaturation persisted for 4 weeks[45] maximum particle number densities of about 6×10^{-6} cm^{-3} are obtained. These particle number densities are up to 3 orders of magnitude lower than the particle number densities observed in the polar stratosphere.[7−9]

The following two main conclusions can be drawn from this work:

(1) It has been shown that the suggested parametrization of pseudoheterogeneous nucleation is erroneous for stratospheric applications. It is in disagreement with thermodynamics and previous HNO_3/H_2O nucleation data. In addition, the newly, experimentally obtained pseudoheterogeneous nucleation rate coefficients are 5 orders of magnitude lower than the values derived by using the parametrization under stratospheric relevant conditions. For this reason, this parametrization should not be used in stratospheric modeling studies.

(2) The analysis of various laboratory nucleation studies with respect to a pseudoheterogeneous nucleation mechanism yields maximum NAD particle production rates which are 3 orders of magnitude lower than the minimum production rates necessary to explain the large nitric acid containing particles and subsequent denitrification observed in the polar stratosphere. Pseudoheterogeneous nucleation cannot be excluded as a possible particle formation mechanism; however, it is not sufficient to explain the particle number densities observed in the stratosphere.

This study and the work of Knopf et al.[21] show that the homogeneous and pseudoheterogeneous nucleation of NAD in STS droplets is not sufficient to explain the large nitric acid containing particles observed in the polar stratosphere. For this reason, it is most likely that heterogeneous nucleation of NAD and NAT on an insoluble particle must be involved as discussed in other studies.[4,47−50] It should be emphasized that the presented data do not rule out the possibility of a pseudoheterogeneous nucleation mechanism. However, in the case of NAD nucleation, the mechanism is not sufficient to explain the particle observations in the polar stratosphere. Pseudoheterogeneous nucleation may be an important nucleation mechanism in other liquid particle systems or for other atmospheric conditions and warrants further investigation.

Acknowledgment. D.A.K. is grateful for helpful discussions with A. K. Bertram, T. Koop, and T. Peter.

References and Notes

(1) Schreiner, J.; Voigt, C.; Kohlmann, A.; Arnold, F.; Mauersberger, K.; Larson, N. *Science* **1999**, *283*, 968−970.
(2) Voigt, C.; et al. *Science* **2000**, *290*, 1756−1758.
(3) Schreiner, J.; Voigt, C.; Weisser, C.; Kohlmann, A.; Mauersberger, K.; Deshler, T.; Kröger, C.; Rosen, J.; Kjome, N.; Larsen, N.; Adriani, A.; Cairo, F.; Di Donfrancesco, G.; Ovarlez, J.; Ovarlez, H.; Dörnbrack, A. *J. Geophys. Res.* **2003**, *108*, 8313.
(4) Voigt, C.; Schlager, H.; Luo, B. P.; Dörnbrack, A.; Roiger, A.; Stock, P.; Curtius, J.; Vössing, H.; Borrmann, S.; Davies, S.; Konopka, P.; Schiller, C.; Shur, G.; Peter, T. *Atmos. Chem. Phys.* **2005**, *5*, 1371−1380.
(5) Worsnop, D. R.; Fox, L. E.; Zahniser, M. S.; Wofsy, S. C. *Science* **1993**, *259*, 71−74.
(6) Fox, L. E.; Worsnop, D. R.; Zahniser, M. S.; Wofsy, S. C. *Science* **1995**, *267*, 351−355.
(7) Fahey, D. W.; et al. *Science* **2001**, *291*, 1026−1030.
(8) Northway, M. J.; Gao, R. S.; Popp, P. J.; Holecek, J. C.; Fahey, D. W.; Carslaw, K. S.; Tolbert, M. A.; Lait, L. R.; Dhaniyala, S.; Flagan, R. C.; Wennberg, P. O.; Mahoney, M. J.; Herman, R. L.; Toon, G. C.; Bui, T. P. *J. Geophys. Res.* **2002**, *107*, 8298.
(9) Brooks, S. D.; Garland, R. M.; Wise, M. E.; Prenni, A. J.; Cushing, M.; Hewitt, E.; Tolbert, M. A. *J. Geophys. Res.* **2003**, *108*, 4487.
(10) Tabazadeh, A.; Djikaev, Y. S.; Hamill, P.; Reiss, H. *J. Phys. Chem. A* **2002**, *106*, 10238−10246.
(11) Djikaev, Y. S.; Tabazadeh, A.; Hamill, P.; Reiss, H. *J. Phys. Chem. A* **2002**, *106*, 10247−10253.
(12) Tabazadeh, A.; Djikaev, Y. S.; Reiss, H. *Proc. Natl. Acad. Sci.* **2002**, *99*, 15873−15878.
(13) Tabazadeh, A. *Atmos. Chem. Phys.* **2003**, *3*, 863−865.
(14) Kay, J. E.; Tsemekhman, V.; Larson, B.; Baker, M.; Swanson, B. *Atmos. Chem. Phys.* **2003**, *3*, 1439−1443.
(15) Koop, T. *Z. Phys. Chem.-Int. J.* **2004**, *218*, 1231−1258.
(16) Khvorostyanov, V. I.; Curry, J. A. *J. Phys. Chem. A* **2004**, *108*, 11073−11085.
(17) Chushak, Y. G.; Bartell, L. S. *J. Phys. Chem. B* **1999**, *103*, 11196−11204.
(18) Turner, G. W.; Bartell, L. S. *J. Phys. Chem. A* **2005**, *109*, 6877−6879.
(19) Stöckel, P.; Weidinger, I. M.; Baumgärtel, H.; Leisner, T. *J. Phys. Chem. A* **2005**, *109*, 2540−2546.
(20) Duft, D.; Leisner, T. *Atmos. Chem. Phys.* **2004**, *4*, 1997−2000.
(21) Knopf, D. A.; Koop, T.; Luo, B. P.; Weers, U. G.; Peter, T. *Atmos. Chem. Phys.* **2002**, *2*, 207−214.
(22) Koop, T.; Biermann, U. M.; Luo, B.; Crutzen, P. J.; Peter, T. *Geophys. Res. Lett.* **1995**, *22*, 917−920.
(23) Koop, T.; Luo, B. P.; Biermann, U. M.; Crutzen, P. J.; Peter, T. *J. Phys. Chem. A* **1997**, *101*, 1117−1133.
(24) Bertram, A. K.; Sloan, J. J. *J. Geophys. Res.* **1998**, *103*, 3553−3561.
(25) Bertram, A. K.; Sloan, J. J. *J. Geophys. Res.* **1998**, *103*, 13261−13265.
(26) Bertram, A. K.; Dickens, D. B.; Sloan, J. J. *J. Geophys. Res.* **2000**, *105*, 9283−9290.
(27) Salcedo, D.; Molina, T.; Molina, M. J. *J. Phys. Chem. A* **2001**, *105*, 1433−1439.
(28) Rivière, E. D.; Terao, Y.; Nakajima, H. *J. Geophys. Res.-Atmos.* **2003**, *108*, 4718.
(29) Drdla, K.; Browell, E. V. *J. Geophys. Res.-Atmos.* **2004**, *109*, D10201.
(30) Larsen, N.; Knudsen, B. M.; Svendsen, S. H.; Deshler, T.; Rosen, J. M.; Kivi, R.; Weisser, C.; Schreiner, J.; Mauerberger, K.; Cairo, F.; Ovarlez, J.; Oelhaf, H.; Spang, R. *Atmos. Chem. Phys.* **2004**, *4*, 2001−2013.
(31) Irie, H.; Pagan, K. L.; Tabazadeh, A.; Legg, M. J.; Sugita, T. *Geophys. Res. Lett.* **2004**, *31*, L15107.
(32) Grooss, J. U.; Günther, G.; Müller, R.; Konopka, P.; Bausch, S.; Schlager, H.; Voigt, C.; Volk, C. M.; Toon, G. C. *Atmos. Chem. Phys.* **2005**, *5*, 1437−1448.
(33) Svendsen, S. H.; Larsen, N.; Knudsen, B.; Eckermann, S. D.; Browell, E. V. *Atmos. Chem. Phys.* **2005**, *5*, 739−753.
(34) Pagan, K. L.; Tabazadeh, A.; Drdla, K.; Hervig, M. E.; Eckermann, S. D.; Browell, E. V.; Legg, M. J.; Foschi, P. G. *J. Geophys. Res.-Atmos.* **2004**, *109*, D04312.
(35) Disselkamp, R. S.; Anthony, S. E.; Prenni, A. J.; Onasch, T. B.; Tolbert, M. A. *J. Phys. Chem.* **1996**, *100*, 9127−9137.
(36) Anthony, S. E.; Onash, T. B.; Tisdale, R. T.; Disselkamp, R. S.; Tolbert, M. A.; Wilson, J. C. *J. Geophys. Res.* **1997**, *102*, 10777−10784.
(37) Prenni, A. J.; Onasch, T. B.; Tisdale, R. T.; Siefert, R. L.; Tolbert, M. A. *J. Geophys. Res.-Atmos.* **1998**, *103*, 28439−28450.

(38) Tabazadeh, A. *Atmos. Chem. Phys. Discuss.* **2003**, *3*, 827−833.
(39) Djikaev, Y. S.; Tabazadeh, A. *J. Phys. Chem. A* **2004**, *108*, 6513−6519.
(40) Pruppacher, H., R.; Klett, J. D. *Microphysics of Clouds and Precipitation*; Kluwer Academic Publishers: Dordrecht, The Netherlands, 1997.
(41) Schnitzer, C.; Baldelli, S.; Campbell, D. J.; Shultz, M. J. *J. Phys. Chem. A* **1999**, *103*, 6383−6386.
(42) Carslaw, K. S.; Luo, B.; Clegg, S. L.; Peter, T.; Brimblecombe, P.; Crutzen, P. J. *Geophys. Res. Lett.* **1994**, *21*, 2479−2482.
(43) Barton, N.; Rowland, B.; Devlin, J. P. *J. Phys. Chem.* **1993**, *97*, 5848−5851.
(44) Dye, J. E.; Baumgardner, D.; Gandrud, B. W.; Kawa, S. R.; Kelly, K. K.; Loewenstein, M.; Ferry, G. V.; Chan, K. R.; Gary, B. L. *J. Geophys. Res.* **1992**, *97*, 8015−8034.
(45) Tabazadeh, A.; Jensen, E. J.; Toon, O. B.; Drdla, K.; Schoeberl, M. R. *Science* **2001**, *291*, 2591−2594.
(46) Mann, G. W.; Davies, S.; Carslaw, K. S.; Chipperfield, M. P.; Kettleborough, J. *J. Geophys. Res.* **2002**, *107*, 4663.
(47) Biermann, U. M.; Presper, T.; Koop, T.; Mösinger, J.; Crutzen, P. J.; Peter, T. *Geophys. Res. Lett.* **1996**, *23*, 1693−1696.
(48) Bogdan, A.; Kulmala, M. *Geophys. Res. Lett.* **1999**, *26*, 1433−1436.
(49) Bogdan, A.; Molina, M. J.; Kulmala, M.; MacKenzie, A. R.; Laaksonen, A. *J. Geophys. Res.* **2003**, *108*, 1371−1380.
(50) Curtius, J.; Weigel, R.; Vössing, H.-J.; Wernli, H.; Werner, A.; Volk, C.-M.; Konopka, P.; Krebsbach, M.; Schiller, C.; Roiger, A.; Schlager, H.; Dreiling, V.; Borrmann, S. *Atmos. Chem. Phys.* 2005.